Use of Distribution Network Topological Fractality and Sunburst Charts in the Online Risk Assessment

Jonatas B. Leite and Jose R. S. Mantovani
Dep. of Electrical Engineering
São Paulo State University - UNESP
Ilha Solteira, Brasil
mant@dee.feis.unesp.br

Mladen Kezunovic
Dep. of Electrical and Computer Engineering
Texas A&M University
College Station, USA
kezunov@ece.tamu.edu

***Abstract*—The integration of outage records, historical weather information and fault management events are used in a risk-based GIS driven proactive management tool. It enables the operator to visualize the hourly risk prediction by the graphical representation of the feeder section with a color to each corresponding risk level. The addition of daily hours to the set of spatial coordinates is well suited to perform online risk mitigation but also increases the visualization complexity. Outputs from the risk assessment must be simple and very informative to promote fast action by control center operators. The simplification step is to use a fractal network approach, which allows the use the box-counting method and the renormalization process where a distribution network is collapsed to one node. This simple node can aggregate information of the whole network by using a circle diagram in form of sunburst chart for dynamic visualization and navigation. The effectively of the designed visualization tool is evaluated under electricity networks from a real-world distribution system.**

***Index Terms*--power distribution networks, geographic information systems, fractality, renormalization, sunburst.**

I. INTRODUCTION

The use of risk reduction control can prevent failures and mitigate consequences through pro-active risk management and affective ranking of risk reduction measures [1]. The weather-based risk assessment allows the risk measurement through the correlation between the weather data and historical management data. The predicted risk level should then be presented to the operator efficiently and timely. The use of single line diagrams may slow down the decision process since some time is needed for the operator to understand the distribution network topological diagram. A fast way to output the monitoring parameters can be achieved by the network clusterization and renormalization where all information can be collapsed into a single point.

During the clusterization procedure a requirement is to determine the number of clusters that is not trivial to select. In the recent literature, the distribution network topologies are studied to find intrinsic properties that improve the underlining mathematical models. In [2], techniques from complex network analysis and graph theory under real-world medium-voltage power grids are used. Among the graph properties, the self-similarity arises as a property of distribution network that repeats graphs patterns over all scales. This is a typical property of fractals. Since the clustering coefficient of medium- and low-voltage distribution networks are zero, the fractal dimension is thus an attractive parameter in the determination of the clusters' number for all zoom scales making the information synthesis more effective.

The fractal geometry of urban growth in [3] is used in a power-law distribution with fractal exponent for simulating the load density growth in a distribution utility service zone. A grid covers a metropolitan area and the electrical loads are grouped per cell without take into account the distribution network topology. On the other hand, [4] assumes the fractal characteristic of electrical power system networks and calculates the fractal dimension of five networks, from IEEE 14 bus system to IEEE 300 bus system. In addition to the determination of fractal dimension of several electricity networks, [5] states that: the larger the electric power network fractal dimension, the greater the opportunity that power system fault may occur. The fractal property is also used by [6] in the creation of virtual distribution networks able to test different scenarios and algorithms without having to collect and process the real-world network data. More recently, the Fractal Grid project [7] addresses the increased complexity of future power grid by developing a multi-scale methodology for smart grids based on fractality where a more flexible, controllable, resilient and interoperable electrical system enable efficient and safe operation.

The distribution network topological fractality can be made useful in a multi-scale framework through the clusterization technique with renormalization concept for creating hierarchical graphs. Reference [8] uses nodes and edges to represent the electricity network. Each edge assumes values of electrical properties of lines, such as admittance or average power flows. In this way, a hierarchical spectral clustering methodology reveals the internal connectivity structure being measured by subgraph volume, boundary and

This work was fully supported by the São Paulo Research Foundation – FAPESP (grant: 2015/17757-2 and 2015/21972-6), CAPES and CNPq (grant: 305318/2016-0).

978-1-5386-8218-0/19/$31.00 ©2019 IEEE

expansion. A modified admittance matrix is also employed by [9] in the determination of a normalized similarity matrix. Then the first k eigenvectors are calculated and clustered by K-means algorithm. The separation of whole network into local areas is necessary for an efficient modeling of large-scale electrical grid. Due to the clusterization necessity and taking the advantage of network topological fractality, [10] proposes a power-grid-partitioning optimization method able to reduce the fault current level of electricity grids by changing the structures of power grids according to fractal dimension.

Our work aims to correlate the fractal dimension of real-world distribution networks with the cluster number for each zoom scale. Thus, a hierarchical graph can be achieved as a multi-scale navigation framework. The information of interest for each layer is collapsed using the sunburst chart that has the capability to show hierarchical layers in a single point. The main contribution of the proposed methodology is the use fractal dimension to create a multi-scale navigation framework embedded into a sunburst chart.

The paper organization is as follows. Section II provides some relevant concepts of fractal geometry, introduces the mathematical formulation of fractal dimension and presents the box counting method applied in distribution networks. Section III depicts the K-means algorithm for finding self-similar functional cuts with minimized disconnection. Section IV relates the hierarchical graph with sunburst chart in a multi-scale navigation framework. Section V discusses the results from the test of the proposed methodology under a real-world distribution system. Section VI lists paper contributions.

II. Fractal Dimension of Electricity Networks

Geometric shapes that show the exactly self-similarity on infinite scales are considered ideal fractals easily observed using the modern computers. The notion of self-similarity in natural shapes and objects sheds lights in understanding natural geometry. The more one zooms in, more similar features are observed. Since natural fractals show statistical self-similarity it means as one zooms in, statistically/ approximately self-similar shapes emerge. It is possible to say that electricity networks present a simplistic kind of self-similarity. If the graph representing a distribution network is cut, the resulting subgraphs will resemble the parent graph in a statistical way. Since the self-similarity is a typical property of fractals, in some networks it is unraveled through the determination of the fractal dimension.

A. Fractal Dimension

The volume of a fractal (or any object), $Vol(s)$, is measured by putting a d-dimensional hypercubic lattice of lattice space s at the same region of space where the object is localized.

$$Vol(s) = N(s)s^d \tag{1}$$

In (1), $N(s)$ is the number of boxes of volume s^d which overlap with the structure and s is much smaller than the linear size L of whole structure. To be able to identify the correct dimension of fractals another non-Euclidian value for d is needed. In nature there are objects so complicated that their dimension is not integer and therefore does not belong to any of the well-known integer dimension of Euclidian geometry. The fractal dimension, D_C, is the value of d for which the volume $Vol(s)$ attains a constant value $M(0 < M < \infty)$, when $s \to 0$ and $N(s) \to \infty$. Substituting $Vol(s)$ with M in (1):

$$N(s) = Ms^{-D_C}, with\ s \to 0, N(s) \to \infty \tag{2}$$

Then the dimension D_C is given by taking the *log* of (2).

$$D_C = \lim_{s\to 0} \frac{\log N(s)}{-\log s} = \lim_{s\to 0} \frac{\log N(s)}{\log 1/s} \tag{3}$$

Because the term $\log(M)/\log(s)$ tends to zero at the limit $s \to 0$, once M is a finite number and $\log(s)$ tends to be infinite. The state-of-art algorithms for estimating the fractal dimension is based on box-counting schemes that quantifies the rate at which an object's geometric details develop at increasing fine scales [11].

B. Box Counting Method

From the formal definition, in which $\log N(s) \sim D_C \log(s)$, and by the assumption of a database with self-similarity in the ranges scales $[r_1, r_2]$, the correlation fractal dimension, D_C, for this range is measure as given by (4).

$$D_C \equiv \frac{\partial \log \sum_i A_i^2}{\partial \log(r)}, r \in [r_1, r_2] \tag{4}$$

Where A_i is the occupancy of the i[th] cell when the address space is embedded into a two-dimensional grid with cells' grid of side r. Fractal dimension algorithm imposes grids of different resolutions over the dataset, starting from the coarsest one to the finest one, and counts the cells' occupancies in order to create the $\log(r) - \log(S(r))$ plot, as shown in Algorithm 1.

Algorithm 1. Get the fractal dimension, D_C, of a dataset.

1: **for** each grid of size $r = 1/2^j$, $j = 1,2,...,|R|$ **do**
2: **for** each point in the dataset **do**
3: Decide which grid cell falls in (i.e. the i-th cell)
4: Increment the counter A_i
5: **end for**
6: Compute de sum of occupancies $S(r) = \sum A_i^2$
7: **end for**
8: Generate a plot using the values of $\log(r)$ and $\log(S(r))$
9: Return the slope of the plot (liner regression) as D_C.

The box counting algorithm can be improved by reversing the sequence of grid granularities, i. e. starting by filling in the occupancies of the finest grid and proceed, consecutively, with coarser-resolution grids [12].

III. Self-Similar Cuts in Distribution Networks

The topological fractality stands for a power-law relation between the minimum number boxes needed to cover the

entire network and the size of the boxes. By controlling the zoom factor into a multi-scale navigation framework, the size of the boxes is controlled as well. The power-law relation provides thus the minimum number of boxes that cover self-similar portions from the entire network. The matching among network nodes and their boxes can be achieved by using clusterization methods.

A. K-means Clustering Method

The K-means algorithm is an iterative optimization method to find the cluster configuration $\boldsymbol{C} = \bigcup_{j=1}^{K} \boldsymbol{C_j}$, where $\boldsymbol{C_j}$ is the set of all network nodes in j[th] cluster, that minimizes the sum of squared Euclidian distance $d_2(\boldsymbol{x_i}, \boldsymbol{m_j})$ between the nodes $\boldsymbol{x_i}$ and their corresponding center $\boldsymbol{m_j}$ [13].

$$\boldsymbol{C^0} = \arg\min_{\boldsymbol{C}} \sum_{j=1}^{K} \sum_{m \in \boldsymbol{C_j}} d_2(\boldsymbol{x_m}, \boldsymbol{m_j})^2 \quad (5)$$

In every iteration t, the reassignment of all nodes to their new cluster is alternated as in (6).

$$\boldsymbol{C_j^t} = \left\{ \boldsymbol{x_i} \middle| d_2(\boldsymbol{x_i}, \boldsymbol{m_j^t}) \le d_2(\boldsymbol{x_i}, \boldsymbol{m_{j'}^t}), \forall j' = 1,2,...,K \right\} \quad (6)$$

Until the convergence, all new cluster centers are recalculated as well.

$$\boldsymbol{m_j^t} = \frac{1}{\left| \boldsymbol{C_j^t} \right|} \sum_{\boldsymbol{x_j} \in \boldsymbol{C_j^t}} \boldsymbol{x_j} \quad (7)$$

The algorithm is initialized by choosing K random points into the two-dimensional space that cover the entire network as initial cluster centers, $\boldsymbol{m_j^0}$. Since the number of clusters depends upon the complexity of the network, this work proposes the use of the power-law.

$$K = \left\lfloor \left(P_{factor} \right)^{D_C} + 1/2 \right\rfloor \quad (8)$$

Equation (8) correlates the network cluster number with its fractal dimension whenever a constant zoom factor P_{factor} is known.

B. Removing Disconnected Cuts

As the distribution network is dealt with as a graph $G(\boldsymbol{V}, \boldsymbol{E})$, then the network portion in every cluster is a subgraph. The K-means algorithm builds the clusters using a two-dimensional vector, $\boldsymbol{X}$, that has the normalized geographical position, latitude and longitude, for each node of the network graph $\boldsymbol{X} = \left\{ \boldsymbol{x_i} \middle| \left(x_i^0, x_i^1 \right) = \left(v_i^{lat}, v_i^{lon} \right) \wedge v_i \in \boldsymbol{V} \right\}$. The use of geographical position vector has poor topological information which increases the probability of clustered subgraphs being disconnected where clusters can have one or more subgraphs.

The positional structure of a graph does not capture the entire functional information about the power distribution grid. The use of edge weights includes this information, where the graph edges' set is the distribution lines set. The edge weights can be interpreted as a penalty for cutting the corresponding line when clustering. It measures the connection strength, as strongly connected vertices are more likely to be clusterized togheter. In these terms, the connectivity information can be described by the nodal impedance matrix, $\boldsymbol{Z^{bus}}$, that reveals the electrical distance among all network nodes.

$$\boldsymbol{X_{new}} = \boldsymbol{X} \cup diag(\boldsymbol{Z^{bus}}) = \left\{ (v_i^{lat}, v_i^{lon}, z_{ii}) \middle| v_i \in \boldsymbol{V} \right\} \quad (9)$$

In (9), the new vector $\boldsymbol{X_{new}}$ is three-dimensional, which implies in the use of normalized spherical coordinates to place initial clusters centers $\boldsymbol{m_j^0}$.

C. Functional Cuts

Although the use of the nodal impedance matrix can improve the connectivety of clusters, there are some functional issues of the distribution system that this information can not cover. One of them is the power distribution feeder sections configuration. As it is desired to have one connected subgraph per cluster, it is desired the clusters have entire distribution feeder sections, as well. This arrangement enables the enclosing of damaged distribution feeder sections by just one cluster. The achievement of more functional clusters comes from their boundaries that must be composed by inter-section devices such as the sectionalizing switches.

$$diag(\boldsymbol{Z_{new}^{bus}}) = \{ z_{ii}^{new} \mid z_{ii}^{new} = z_{jj}^{new} + z_{ji}^{pri} + \beta_{ji}, e_{ji} \in \boldsymbol{E} \} \quad (10)$$

$$\beta_{ji} = \begin{cases} \max_{diag(\boldsymbol{Z^{bus}})} \{ z_{ii} \} / n_{FS}, & if\ e_{ji} \in \boldsymbol{E} \wedge e_{ji} \in \partial \boldsymbol{SG_{FS}} \\ 0, & otherwise \end{cases} \quad (11)$$

Equation (10) expresses the modification in the calculation of the diagonal elements from the nodal impedance matrix. When the edge has vertices in different feeder sections, it belongs to the section boundary, $e_{ji} \in \partial \boldsymbol{SG_{FS}}$, and its primitive impedance, z_{ji}^{pri}, is added to β_{ij} increasing the electrical distance among nodes at different sections. With this information, the K-means algorithm must provide clusters where their boundaries match to distribution feeder section boundaries.

IV. Appling Topological Fractality in Online Risk Assessment

In a typical renormalization, the entire network is covered with boxes, here clusters. In this way, the renormalized network is built by replacing each box by supernodes (or renormalized nodes) and these nodes are connected if there is at least one link between two nodes in their corresponding boxes. When the renormalization is applied to a self-similar network, it leads to a new network that presents similar properties as the parent one. For example, in Fig. 1 (a) the supernode "0" covers the nodes "00", "01" and "02" that are connected similarly to main network of supernodes. This is a hierarchical scale free graph like a fractal structure.

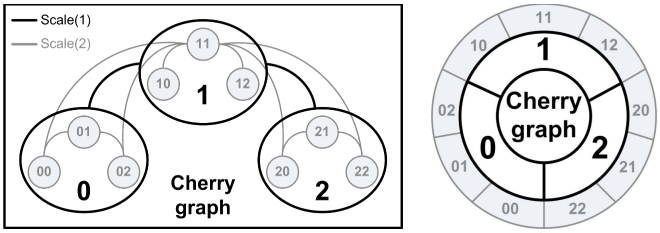

(a) (b)

Figure 1 Renormalization procedure: (a) hierarchical scale free graphs [14] and (b) graph synthesis on sunburst chart.

The information of interest in every node of the hierarchical graph can be represented using a sunburst chart. In Fig. 1 (b), the caption of every node is presented in the sunburst chart. The main square is in the central cycle providing global information of the graph. Middle cycle has the supernodes information at the first scale while the external cycle displays information of the second scale nodes. Thus, this work takes the risk level from the online risk assessment [15] as the information of interest to show in the sunburst chart.

$$R_p = \max_{v_i \in G_p} \{R(v_i)\},\ p = 0,1,...,n_{scale} \qquad (12)$$

In (12), the risk level, R_p, for each scale p is achieved as the maximum risk level among all nodes, or clusters, that are visualized in the scale p and comprise the subgraph G_p. In the following section, all theoretical assumptions taken by this work are evaluated using a real-world distribution system with power networks of different topologies.

V. Appling Topological Fractality in Online Risk Assessment

The topologies of real-world distribution networks are shown in figures along this section. The evaluation approach is focused on three main concepts as proposed in the previous methodology sections. Firstly, the calculation of the fractal dimension to distribution network is verified. Then, the evaluation of the clustering method is done as well as the techniques to improve the self-similar cuts. At last, the visualization of the renormalization process using dynamic sunburst charts is applied to represent online risk assessment.

A. Fractal Dimension of RealDistribution Network

Figure 2 displays two topologies of MV power networks from the real-world distribution system. The network in Fig. 2 (a) has many lateral branches looking like a tree while the other one, in Fig. 2 (b), looks like a single long line with few lateral branches. This topological difference is mathematically observed through the calculation of the fractal dimension as is illustrated in Fig. 2 (c) with the liner regression for each network. The slope, or fractal dimension, of the network in (a) is equal to 1.3366 which is greater than the slope of the network in (b), that is 1.116. This indicates the network in (a) is topologically more complex and, as consequence, it need be clustered with a larger number of clusters. Thus, the number of clusters to the network in (a) is equal to K_A=*3* while the network in (b) can be clustered using K_B=*2* clusters.

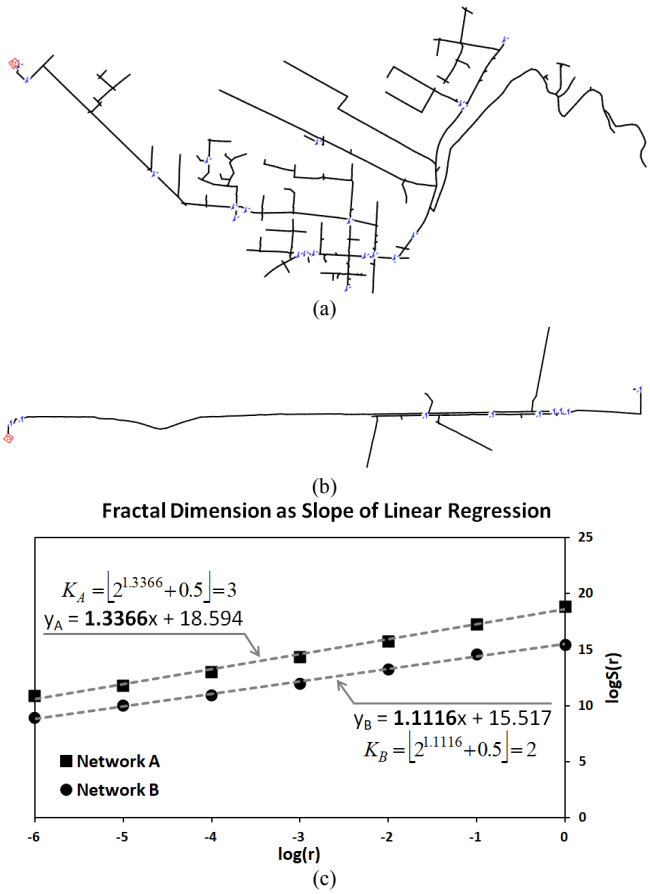

Figure 2 Fractal dimension in different distribution networks: (a) and (b) example of real-world MV power networks, (c) charts of linear regression.

B. Self-Similar Cuts

With the achieved number of clusters the K-means algorithm performs the clusterization by splitting the whole network in subgraphs. Ideally, each cluster must cover one connected subgraph, but just using geographical coordinates it is not always possible. In the Fig. 3 (a), the clustering is obtained by using a dataset with the georeferenced information for each node of the network. As the clustering result, the blue cluster cover correctly one connected graph, G_0^{blue}. On the other side, the red cluster has two subgraphs, i.e. with one additional disconnected subgraph, G_1^{red}. The proposed way to minimize this effect is the use of the topological information. The insertion of the nodal impedance information into the dataset allows for improving the clustering procedure. Figure 3 (b) displays this improvement where each cluster covers only one connected subgraph.

A MV/LV power network with high fractal dimensionality (Fig. 5(b)) is used in the measurement of additional disconnected subgraphs through every scale, or layers of the hierarchical graph. The bar chart in Fig. 3 (c) compares the number of disconnected graph for each hierarchical node. The global power network is represented by the hierarchical node 1. Using the dataset with two geographical coordinates (2d DS), the clusterization yields 7 additional disconnected

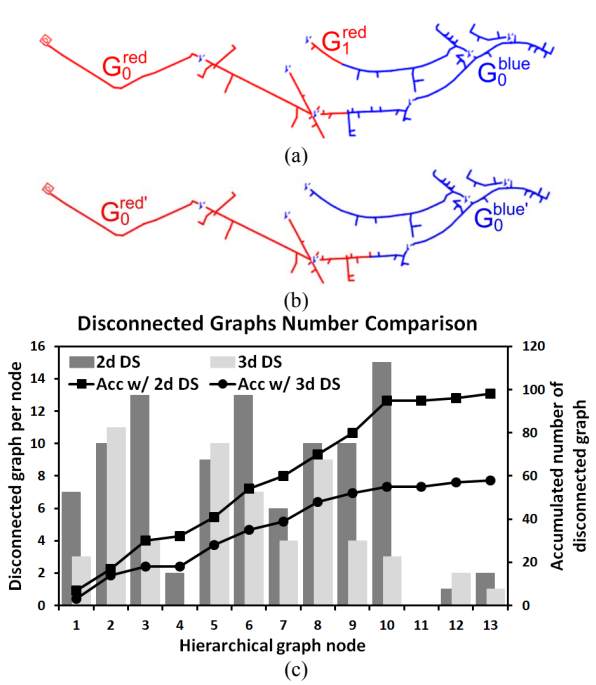

Figure 3 Subgraphs provided by the clustering algorithm: (a) by dataset with geographical coordinates, (b) addition of nodal impedance in the dataset and (c) charts with the compared number of additional disconnected subgraghs in a real-worf MV/LV power network.

graphs, while inserting the nodal impedance information into dataset (3d DS), the number of disconnected graphs decreases to 3. In general the number of additional disconnected graph reduces when the nodal impedance information is inserted into dataset. This reduction is measured by the accumulated number of the disconnected graph in all hierarchical nodes. The chart in Fig. 3 (c) shows that the line of accumulated disconnected graphs with nodal impedance (Acc w/ 3d DS) is below the line of accumulated disconnected graphs with just geographical coordinates (ACC w/ 2d DS). The total reduction is around 40% and can be improved by manipulating the nodal impedance as in the proposed functional cuts.

The architectural structure of distribution networks provides resources to perform functions like the network reconfiguration during the power restoration procedures. Sectionalizing switches (SW) are installed along the distribution network to enable this function. Thus, it is useful for the clusters' boundaries to have theses sectionalizing devices. The nodal impedance information is modified as given in (10) and (11) to increase the similarity within the clusters for creating more functional cuts. This behavior is verified in the Fig. 4 (a), (b) and (c) where the clusters at three first layers of the hierarchical graph are observed. In (a) the switches SW_1 and SW_5 comprise the boundaries of the red clusters, G_{00}^{red}, at the 1st layer. In (b), the boundaries of G_{01}^{red} has the SW_1 and SW_2. In (c), the red cluster G_{02}^{red} is bounded by switches SW_2 and SW_4. Other benefit of the functional cuts is the reduction in the number of additional disconnected graphs as shown in Fig. 4 (d) where the reduction reaches 60%.

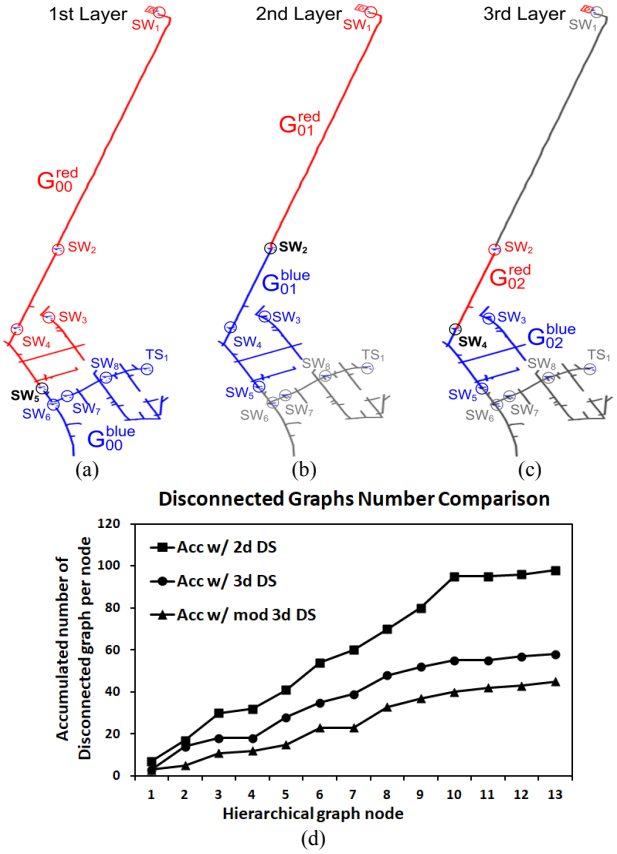

Figure 4 Cluterization of a power network: (a) 1st layer, (b) 2nd layer, (c) 3rd layer and (d) line charts with accumulated disconnected charts.

C. *Dynamic Sunburst Charts and Network Navigation*

The proposed sunburst chart approach to online risk assessment is evaluated under a real-world distribution network. The sunburst approach enables an advanced visualization tools across the hierarchical graph. Figure 5 (a) shows the design of this tool to the 1st hierarchical layer where the blue, red and green triangles are navigation buttons with the function to enter into color matching cluster. The sunburst chart display the real-time risk levels, R_p, by using colors tones: the light blue symbolizes low; the olive green symbolizes medium; and the dark red symbolizes high risk level. The central cycle always shows the risk level in global network, the current hour and hierarchical layer visualized, in the case it is the 1st, *HL(1)*. The middle cycle displays the current risk level for each visualized cluster. As the hours and hierarchical layers change, the risk levels at middle cycle change as well. The external cycle maintains the chronology of risk levels per cluster along the daily twenty four hours by starting at zero hour (00:00).

Figure 5 (a) displays the measured risk levels by the online risk assessment procedure. At 08:00, the blue cluster has low risk, the red one has high risk and green has medium risk. The red button is clicked to enter into cluster with high risk. A zoom in factor of two times is performed. The selected cluster is centralized on the screen indicating the navigation to 2nd hierarchical layer as illustrated in Fig. 5 (b). A new clustering is achieved and, consequently, the risk levels displayed in the

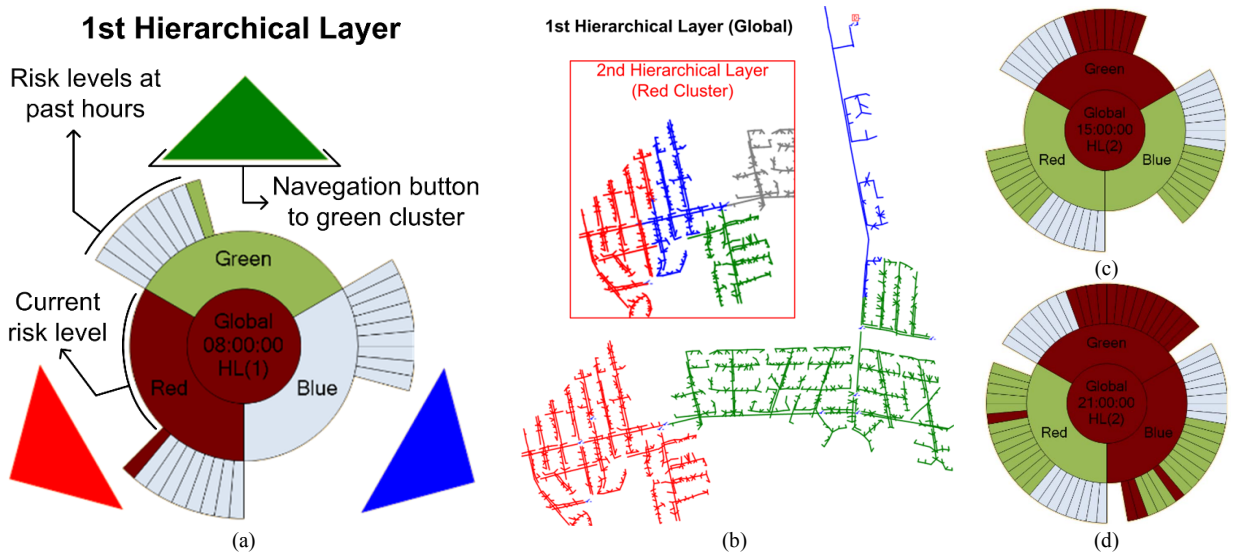

Figure 5 Visualization and navigation for the renormalized distribution network: (a) 1st layer dynamic sunburst chart with navigation buttons; (b) network topologies to 1st and 2nd hierarchical layers; (c) 2nd layer sunburst chart at 15:00; and (d) 2nd layer sunburst chart at 21:00.

sunburst chart also changes, except in the center cycle that always shows the global risk level. Figure 5 (c) displays the updated chart at 15:00 to the 2nd hierarchical layer. By looking in the external cycle, at 08:00 the 2nd layer green cluster has high risk level while the others have medium risk level. This risk levels remained until 15:00. In Fig. 5 (d), the sunburst chart is taken at 21:00 when the high risk level is in 2nd layer green and blue clusters. At the same time, the red cluster has medium risk level but, by looking in the red cluster chronology, at 16:00 its risk level is high as a consequence of severe weather condition.

VI. Concluding Remarks

The following are the paper contributions and future works:

- Using the distribution network topological fractality, the correlation between fractal dimension and number of clusters in a distribution network is defined.
- A multi-scale navigation framework is enabled using the renormalization procedure where the distribution network becomes a hierarchical graph with information of interest displayed as a dynamic sunburst chart.
- The use of dynamic sunburst charts make outputs from the online risk assessment be very informative in order to promote fast insights on network operators at control rooms. The proposed approach should provide a way for comprehension of the current situation into a strategy of situation awareness able to improve the distribution network resiliency.

References

[1] D. Vose, "Risk Analysis: a Quantitative Guide," vol. 1, 3rd ed., West sussex, England: John Wiley & Sons, 2008, 729 pp.

[2] S. Abeysinghe, J. Wu, M. Sooriyabandara, M. Abeysekera, T. Xu & C. Wang, "Topological properties of medium voltage electricity distribution networks," *Applied Energy*, v. 210, pp. 1101-1112, Jan. 2018.

[3] Melo, Joel D., Carreno, Edgar M., Padilha-Feltrin, Antonio & Minussi, Carlos R., "Grid-based simulation method for spatial electric load forecasting using power-law distribution with fractal exponent," *Int. Trans. Electr. Energ. Syst.*, v. 26, pp. 1339-1357, June 2016.

[4] Sai R. Viswanadh & V. Bapi Raju, "Application of Fractals to Power System Networks," *Int. J. Sci. Eng. Tech. Res..*, v. 5, pp. 2547-2553, July 2016.

[5] Hou, H., Tang, A., Fang, H., Yang, X. & Dong, Z., "Electric power network fractal and its relationship with power system fault," *Technical Gazette*, v. 22, n. 3, pp. 623-628, 2015.

[6] F. Barakou, D. Koukoula, N. Hatziargyriou and A. Dimeas, "Fractal geometry for distribution grid topologies," 2015 *IEEE Eindhoven PowerTech*, Eindhoven, 2015, pp. 1-6.

[7] G. Kariniotakis, L. Martini, C. Caerts, H. Brunner, N. Retière, "Challenges, Innovative Architectures and Control Strategies for Future Networks: The Web-of-Cells, Fractal Grids and Other Concepts," *CIRED 2017 - 24th International Conference on Electricity Distribution*, Glasgow, United Kingdom. pp.1287, 2017.

[8] R. J. Sánchez-García et al., "Hierarchical Spectral Clustering of Power Grids," in *IEEE Transactions on Power Systems*, vol. 29, no. 5, pp. 2229-2237, Sept. 2014.

[9] Brato, S., Surmann, D., Krey, S., Götze, J., Ligges, U. & Weihs, C., "Stability Analysis and Clustering of Electrical Transmission Systems", Feb. 2014, DOI: 10.17877/DE290R-13190.

[10] Li, Hongzhong, Zhang, Xinyu, Han, Wenhua, Li, Yingchuang & Kang, Aimin, "A power grid partitioning optimization method based on fractal theory," *Int. Trans. Electr. Energ. Syst.*, Oct. 2018, DOI:10.1002/etep.2741.

[11] C. Traina Jr., A. Traina, L. Wu and C. Faloutsos, "Fast Feature Selection using Fractal Dimension", *J. of Inform. and Data Managem.*, vol. 1, no. 1, pp. 3–16, Feb. 2010.

[12] C. Attikos and M. Doumpos, "Faster Estimation of the Correlation Fractal Dimension Using Box-counting," *2009 Fourth Balkan Conference in Informatics*, Thessaloniki, 2009, pp. 93-95.

[13] MacKay, D. "Chapter 20. An Example Inference Task: Clustering". *in Information Theory, Inference and Learning Algorithms*. Cambridge University Press. pp. 284–292, 2003.

[14] J. Komjáthy, K. Simon, "Generating hierarchial scale-free graphs from fractals," *Chaos, Solitons & Fractals*, vol. 44, no. 8, pp. 651-666, Aug. 2011.

[15] J. B. Leite, J. R. S. Mantovani, T. Dokic, Q. Yan, P. –C. Chen and M. Kezunovic, "Resiliency Assessment in Distribution Networks Using GIS Based Predictive Risk Analytics," in *IEEE Transactions on Power Systems,* (Early Access) DOI: 10.1109/TPWRS.2019.2913090.